

Which causal scenarios are interesting?

Jacques Pienaar*

Faculty of Physics, University of Vienna, Boltzmannngasse 5, A-1090 Vienna, Austria. and
Institute of Quantum Optics and Quantum Information,
Austrian Academy of Sciences, Boltzmannngasse 3, A-1090 Vienna, Austria.

A causal scenario is a graph that describes the cause and effect relationships between all relevant variables in an experiment. A scenario is deemed interesting if different operational probabilistic theories give rise to different marginal distributions of the observed variables – a Bell-type experiment is one example. Graphs that are not interesting are boring in a precise sense: the predictions of an arbitrary generalised probabilistic theory (quantum or otherwise) can be reproduced by local hidden variables respecting the causal structure of the graph. Henson, Lal and Pusey (HLP) recently proposed a sufficient condition for a causal scenario to be boring. In this paper we review and propose several sufficient conditions for a graph to be interesting. We first show that existing graphical techniques due to Evans can be used to confirm that many graphs are interesting without having to explicitly search for inequality violations. For three exceptional cases – the graphs numbered #15, 16, 20 in HLP – we show that there exist non-Shannon type entropic inequalities that imply these graphs are interesting.

I. INTRODUCTION

Every physical experiment has an underlying causal structure, conceived of as a series of *events*, and the *influences* they have on each other. Just as trees look much the same when stripped of their leaves, it is possible for experimental set-ups in widely differing contexts to nevertheless exhibit the same causal structure. Causal structure is a useful abstraction that permits us to classify experiments by their cause-and-effect relationships, ignoring the unnecessary details of their physical implementation.

In this spirit, even a complicated physical system has a simple representation in terms of a directed acyclic graph (DAG) describing its causal structure, like that of the bicycle shown in Fig 1. In this graph (called the *causal graph*), the triangular nodes represent the minimal set of observed events that are needed to describe the outcomes of experimental probing of the bicycle. Circular nodes represent *unobserved variables*, which are not directly measured but can affect the observed outcomes. The arrows indicate direct causal influences between events. The probabilities for the values of observed variables are governed by a set of functions relating each variable to its direct causes in the graph; these functions are called the *model parameters*. A causal graph dressed with a set of model parameters is called a *causal model* [1, 2].

Following Ref. [3], a causal graph containing both observed and unobserved nodes is called a *generalized DAG* (GDAG). In general, the unobserved variables in a GDAG can represent other objects besides random variables, such as quantum states or even ‘black boxes’ from some hypothetical theory beyond quantum mechanics. Traditionally, however, the unobserved nodes are just random variables whose values are marginalised (summed

over), in which case they are called *latent variables*. In this case, the causal model is called *classical*.

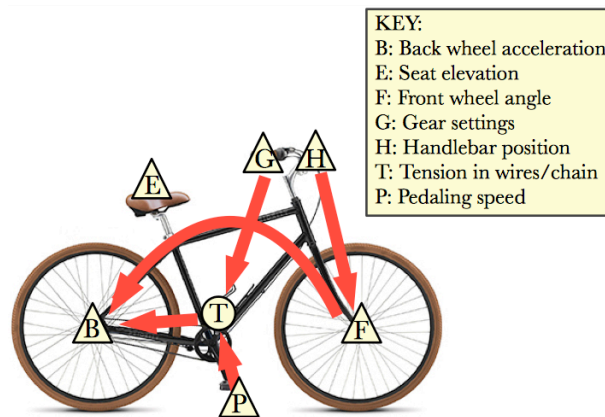


FIG. 1. A causal graph describing the functioning of a bicycle. The gear settings G (including brakes) and the pedalling speed P influence the acceleration vector B of the back wheel, via the tension T in the wire cables and in the bicycle chain. Since the tension is not directly visible to the eye, we consider it a latent variable. The handlebar position H influences the direction of B indirectly, via its influence on the front wheel orientation F . The direct influence of F on B is made possible by the frame of the bicycle. The seat elevation E is causally unrelated to the other variables, so is represented by an isolated node (such nodes are usually omitted from the graph as irrelevant).

What are causal models good for? A typical scientific experiment consists of observing some phenomenon in the laboratory under controlled and repeatable conditions, and then asking whether the probability distribution of the observed events has an explanation in terms of some known physical theory. A causal model provides us with a formal definition of *explanation*. If we can find a causal model that reproduces the observed probabilities, then we say that the observed phenomenon can be ex-

* jacques.pienaar@univie.ac.at

plained by the model. Hypothesis testing then becomes the work of designing experiments to rule out different competing explanations.

The literature on *causal inference* provides numerous tools for deciding when one causal model is a better explanation than another. In general, simpler explanations are preferable to more complex ones. Explanations should be *faithful*, meaning that the choice of model parameters does not have to be fine-tuned in order to fit the observed independencies. If these principles are not enough to differentiate different hypotheses, it is always possible to do so by performing experimental *interventions*: actively changing the values of some variables and observing the reaction of the remaining variables. A tool of causal inference called the *do-calculus* tells us which interventions are needed to obtain specific information about the causal structure.

It is now known that classical causal models cannot adequately explain experiments in quantum physics, particularly the so-called ‘Bell-type’ experiments [4–6]. This is because quantum physics does not permit us to assign values to properties of a system that are not measured in the same run of the experiment – hence we cannot treat unobserved nodes as latent variables as we do in the classical case. Instead of marginalisation, probabilities must be obtained using the quantum formalism, where systems are described by positive operators on Hilbert spaces and probabilities obtained by the Born rule.

The inadequacy of a classical explanation for Bell-type experiments was traditionally interpreted as the impossibility of a ‘local realistic hidden variable model’. A more recent perspective due to Wood & Spekkens is that there exists no *faithful* classical causal model that explains these experiments [7]. Recent work has therefore sought to define *quantum* causal models, which aim to provide a faithful account of quantum phenomena and thereby enable causal inference in the quantum setting [8–11].

Henson, Lal and Pusey (HLP) [3] showed that it is possible to define more general causal models than quantum causal models. One can consider a causal explanation in terms of any hypothetical *generalised probabilistic theory* (GPT), of which classical and quantum causal models are just special cases. The key to the generalisation lies in how we interpret the unobserved nodes. For a classical causal model, an unobserved node is a latent variable; in a quantum causal model, it represents a quantum resource, such as an entangled state; more generally, it represents a ‘black box’ resource of some GPT.

The recognition that different laws of physics necessitate different frameworks for causal inference leads to the conclusion that what constitutes an *explanation* depends on what model of the physical world we choose to take as primitive. It is especially interesting to ask whether, in an experiment whose causal structure is given, there exist differences between the probability distributions that can be explained by different physical models. An example is the causal structure of Bell-type experiments, shown

in Fig. 2: if this GDAG is dressed with classical model parameters, the probability distributions satisfy *Bell inequalities*; if we use quantum model parameters, the distributions satisfy the weaker *Tsirelson’s bound*[12]; and if we use a GPT that allows *Popescu-Rohrlich boxes*[13], the only relevant bound is the no-signalling constraint.

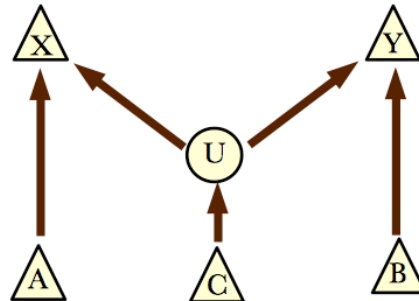


FIG. 2. A causal graph describing a generic Bell-type experiment. A source produces pairs of particles in a state determined by the setting C . A and B are the settings of measurements on each particle, and X, Y are the respective outcomes. These outcomes are influenced by the setting C indirectly via some unobserved node U , typically interpreted as the state of the physical particles produced by the source. Classically, this would be a latent random variable (like the state of the bicycle chain in Fig. 1), but it can represent a quantum state or a more general type of resource as in Ref. [3].

The fact that this same causal graph supports different sets of observed probabilities means that experiments within this causal structure can be used to perform inference *on the laws of physics themselves*. In effect, by assuming that the causal structure has a given form, we are able to distinguish different physical theories within that structure. This is, after all, precisely why Bell-type experiments are commonly interpreted as ruling out classical physics in favour of quantum mechanics. If a resource were ever discovered that could violate Tsirelson’s bound in a Bell-type experiment, this would in turn constitute evidence against the general validity of quantum mechanics. For this reason, the causal graph of this experiment (called the *Bell scenario*) is considered to be ‘interesting’.

Not every causal structure is interesting in this sense. Trivial examples include DAGs in which all variables are observed (these always have a classical explanation), or GDAGs in which all variables share a single common cause (an example of *superdeterminism*). A less trivial example is the so-called ‘one-sided Bell scenario’ (see Fig. 3), in which one of the measurements is fixed (hence not a random variable). In this case, although there is a non-trivial no-signalling constraint imposed by the causal structure (A cannot send signals to Y), it turns out that all possible observed probability distributions can be faithfully reproduced by some choice of classical model parameters. We refer to causal structures like this one as *boring* (not interesting), because experiments

based on them have no hope of differentiating between classical, quantum or supra-quantum theories.

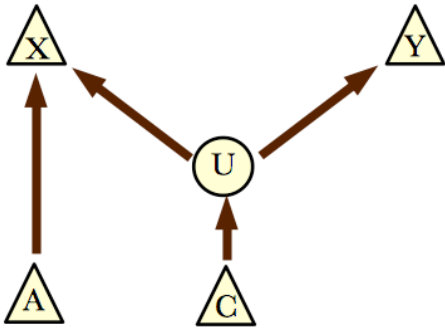


FIG. 3. A causal graph describing a ‘one-sided’ Bell-type experiment. Only one measurement setting A is freely chosen; the other setting is fixed to a particular value and so is not shown in the graph. The graph is *boring*, because it allows a classical explanation regardless of the underlying physical theory. This is also true for variations of the scenario in which the value of B changes in each run but is not ‘freely chosen’; see for example Fig.26(a) in Ref.[7].

The question now arises how to decide whether a given causal graph is boring or interesting. In their paper, HLP introduced a sufficient criterion for a graph to be boring, and conjectured its necessity as well. To provide evidence for this conjecture, they tried to show explicitly that graphs failing their criterion must be interesting, i.e. must allow probability distributions not achievable by any classical causal model. They were able to do this for almost all graphs of up to seven nodes. Only three graphs, labelled # 15,16,21 (see Fig. 7), resisted both the sufficient criterion for boringness *and* the authors’ attempts to find any interesting probability distributions on the graphs. A main result of the present paper is to resolve this impasse.

The method used by HLP to demonstrate interestingness is somewhat tedious, as it requires identifying an explicit constraint (eg. an entropic constraint or algebraic inequality) and then showing that the constraint does not follow from the causal structure alone. Often the best way to achieve this is to find a counterexample – a distribution that violates the constraint in question while satisfying all the causal constraints – but this requires performing an explicit search of the probability space. In this paper, we show that this tedious process can sometimes be sidestepped using known techniques from the literature, and we propose a new method that confirms the interestingness of the graphs # 15,16,21. The new method shows some promise for more general applications, as it is related to the *calculus of interventions* from the literature on causal inference[1].

The paper is organised as follows. Sec. II contains essential notation and background. We then show in Sec. III that some simple graphical methods due to

Evans[14, 15] can be used to confirm the interestingness of a graph by inspection. To illustrate the usefulness of this method, we apply it to the graphs considered by HLP and confirm their results. The only cases that do not satisfy Evan’s sufficient criteria for interestingness are the Bell and Triangle scenarios, and the graphs # 15,16,21. For the latter three, in Sec. IV we propose a novel extension of the methods of entropic inequalities [16–18] that confirms these graphs as interesting (and thereby completes the establishment of HLP’s conjecture for graphs with up to seven nodes). Sec. V contains our conclusions and outlook.

II. DEFINITIONS AND STATEMENT OF THE PROBLEM

In this section we review notation and definitions that will be used in this paper. For a more complete introduction, the reader is referred to Refs. [1, 2] for background on causal models, and to Refs. [16–19] for background on entropic bounds for causal graphs relevant to this paper.

In this work, we are concerned with joint probability distributions $P(A, B, C, \dots)$ of random variables denoted by capital Roman letters A, B, C, \dots . Sets of random variables will also be denoted by capital Roman letters; the context will make it clear whether a letter refers to a single variable or a set of variables. For expressions involving set unions, we omit the ‘ \cup ’, for example $XY := X \cup Y$ is understood. Each variable takes values in a discrete, finite set. Whenever we need to make specific reference to them, we take these values to be positive integers. When talking about a specific joint probability distribution, eg. $P(X, Y, Z)$, we will often represent the marginal distributions of P simply by omitting the relevant variables from P ’s domain; eg. $P(X) := \sum_{Y, Z} P(X, Y, Z)$. A *conditional probability*, denoted $P(X|Y)$ for disjoint sets of variables X, Y , defines a family of probability distributions on the domain of X , parametrized by the discrete index Y . Thus, for example, $P(X|Y = 1)$ and $P(X|Y = 3)$ are two different distributions of the variable X , both belonging to the parametrized family of distributions $P(X|Y)$. The law of total probability relates all these concepts in a simple equation: $P(X, Y) = P(X|Y)P(Y)$.

There are two key properties of joint probability distributions that can be used to characterise them: the *conditional independence (CI)* relations between variables, and the *entropic* relations between the variables. We discuss each of these in turn.

Definition 1: CI relations Let X, Y, Z be three disjoint sets of variables with joint distribution $P(X, Y, Z)$. The sets X and Y are said to be *conditionally independent* given Z , denoted $(X \perp Y|Z)$, iff $P(X|Y, Z) = P(X|Z)$.

Informally, this means that learning the value of Y

provides no new information about the value of X if we already know the value of Z . Given a distribution $P(V)$ on a set of variables V , the set denoted $\text{CI}_P(V)$ contains all conditional independence relations that hold in P between all disjoint subsets of V . Any set of CI relations implies further CI relations via the *semi-graphoid axioms*, which are in turn derivable from the axioms of probability theory. We do not reproduce these here as we will not require them explicitly. A set of CI relations is called *complete* iff it is closed under the semi-graphoid axioms.

Any complete set of CI relations for a set of variables V can be encoded in a DAG whose nodes correspond to the variables in V . CI relations are recovered from the graph using a criterion called *d-separation*:

Definition 2: d-separation Given a DAG for a set of variables V , two disjoint subsets of variables X and Y are said to be *d-separated* by a third disjoint set Z , denoted $(X \perp Y|Z)_d$, iff all undirected paths (i.e. ignoring the direction of arrows) from X to Y are *blocked* by a member of Z . A path is blocked by a member of Z iff:

- (i) the path contains a chain $i \rightarrow m \rightarrow j$ or a fork $i \leftarrow m \rightarrow j$ such that the middle node m is in Z ; or
- (ii) the path contains a collider $i \rightarrow m \leftarrow j$ such that the node m and its descendants are not in Z .

(If there is no path connecting two nodes, as in a disconnected graph, they are trivially d-separated by all other subsets of nodes). By imposing a correspondence between d-separation and CI relations, $(X \perp Y|Z)_d \Rightarrow (X \perp Y|Z)$, every DAG $G(V)$ implies a complete set of CI relations on the variables V , denoted $\text{CI}_G(V)$. Conversely, every complete set of CI relations represents the d-separation relations of at least one DAG.

The link between CI relations and causal models is as follows: any causal model that can serve as an explanation for a distribution $P(V)$ must have a DAG $G(V)$ whose corresponding CI relations $\text{CI}_G(V)$ are a subset of the set $\text{CI}_P(V)$. More generally, we might regard $P(V)$ as a marginal of an unknown distribution $P(V, U)$ and seek an explanation in terms of a GDAG $G(V, U)$ that includes latent variables U . In this case consistency requires that the subset of CI relations $\text{CI}_G(V)$ (i.e. restricted to the observed variables V) should be a subset of the CI relations in the marginal $\text{CI}_P(V)$.

Since our main goal in this work is to classify the possible distributions that can arise from a given GDAG ignoring interventions, we do not review the details of causal inference, although we refer to it in passing in Sec. IV.

We now turn to a different property of probability distributions: the *entropic* constraints between variables. Given any set of variables X distributed by $P(X)$, we can associate an *entropy*, $H(X)$. A common example is

the *Shannon entropy* defined by:

$$H(X) := - \sum_X P(X) \log_2 [P(X)], \quad (1)$$

where the sum is over the values of all variables in X . Given an entropy function, it is also useful to define the *conditional mutual information* of X and Y conditional on Z as:

$$I(X : Y|Z) := H(XZ) + H(YZ) - H(XYZ) - H(Z).$$

Intuitively, this tells us how much the variables X and Y are correlated, conditional on the value of Z . The connection to CI relations is that the causal constraint $(X \perp Y|Z)$ is equivalent to the entropic constraint $I(X : Y|Z) = 0$.

Unless otherwise specified, the results in this work apply to any entropy function that satisfies the *polyamitoidal axioms* (also called *elementary inequalities*). Let V denote a set of variables, $X \subseteq V$ an arbitrary subset, and A, B specific variables in V . Then these inequalities are:

$$\begin{aligned} H(V \setminus A) &\leq H(V), \quad \forall A \in V; \\ H(X) + H(XAB) &\leq H(XA) + H(XB), \quad \forall (A \neq B) \in V \setminus X; \\ H(\emptyset) &= 0. \end{aligned} \quad (2)$$

Any inequality that follows from these is called a *Shannon-type* inequality. Given a set of variables V distributed by $P(V)$, an entropy function assigns a real value ≥ 0 to all subsets of V . If we regard each subset as the basis of an abstract vector space, then the entropy function maps the distribution P to a vector in this space; the set of all such vectors (corresponding to valid probability distributions) defines a convex cone. An explicit description of this cone has not been found to date. However, since all valid entropy functions must satisfy the inequalities (2), these define an outer approximation called the *Shannon cone*. The entropy vector of any valid distribution $P(V)$ must lie within this cone, but the converse is not true – there are sometimes distributions that satisfy all Shannon-type inequalities but cannot be obtained as the marginal of a valid probability distribution on V .

We are now in a position to formally state the problem of whether or not a GDAG is *interesting*. Let $G(V, U)$ be a GDAG with observed variables V and unobserved variables U . We are concerned with the question of whether all distributions $P(V)$ that respect the causal structure of G can arise as the marginal distribution of a classical causal model. Following HLP, let \mathcal{I} be the set of distributions $P(V)$ that respect the observable independencies implied by G , i.e. such that $\text{CI}_G(V) \subseteq \text{CI}_P(V)$. Next, define \mathcal{C} as the set of distributions $P(V)$ that are marginals of some probability distribution $P(V, U)$ having $\text{CI}_G(V, U) \subseteq \text{CI}_P(V, U)$. Since the latter condition is strictly stronger, we have $\mathcal{C} \subseteq \mathcal{I}$, and the graph is called *interesting* if and only if the inclusion is strict, $\mathcal{C} \neq \mathcal{I}$.

(otherwise it is *boring*). Note that a difference between these sets indicates the existence of constraints on \mathcal{C} that can be violated by distributions in \mathcal{I} . Thus, a sufficient condition to show that a GDAG is interesting is to identify a constraint in \mathcal{C} that does not apply in \mathcal{I} . This can be established in two ways: (i) the constraint is excluded from \mathcal{I} by construction, or (ii) the constraint can be shown to be violated by a specific distribution in \mathcal{I} . The first method is simplest (when it applies) and can be done by purely graphical techniques, some of which are reviewed in the next section. The second method requires searching the probability space of \mathcal{I} for suitable counterexamples, but can succeed in many cases where the first method fails; in Sec IV we employ this method using ‘fine grained’ inequalities.

III. THE SKELETON METHOD AND EVANS SEPARATION

In this section, we review two graphical techniques proposed by Evans for identifying cases where $\mathcal{C} \subsetneq \mathcal{I}$, that is, for identifying graphs as interesting. The first technique is called the *Skeleton method*, and the second is called *Evans separation*. We begin with some useful definitions adapted from Refs. [14, 15]. In what follows, $G(V, U)$ is a GDAG with observed variables V and unobserved variables U .

Definition 3: hidden paths and causes.

Let X, Y be any specific variables in G . A directed path from X to Y is called a *hidden path* iff it contains more than one arrow and all nodes on the path besides X, Y are in U (i.e. unobserved). Two variables X, Y are said to share a *hidden common cause* iff they share an unobserved common ancestor $W \in U$ to which they are either directly connected, or connected by a hidden path.

Definition 4: maximal connected subsets.

In the GDAG $G(V, U)$, a subset of observed variables $B \in V$ is called *connected* iff all nodes in B share a single hidden common cause. A connected set B is called *maximal* iff there is no other connected set that fully contains it. Let $\mathcal{B}_G(V)$ denote the set of all maximal connected subsets (of size ≥ 2) in G .

Definition 5: canonical GDAG.

Given the GDAG $G(V, U)$, define its *canonical projection* $G'(V, W)$ as follows:

- (i) The observed nodes of G' correspond to those in G .
- (ii) Two observed nodes X, Y are connected by an arrow $X \rightarrow Y$ in G' iff they are connected by an arrow or a hidden path in G .
- (iii) There is one unobserved node in W for each maximal connected subset of G , and each node in W is a direct cause of all nodes in the corresponding element of $B \in \mathcal{B}_G(V)$.

A GDAG is said to be in *canonical form* iff it is equal to its own canonical projection. Fig. 4 shows an example of the canonical projection of a GDAG.

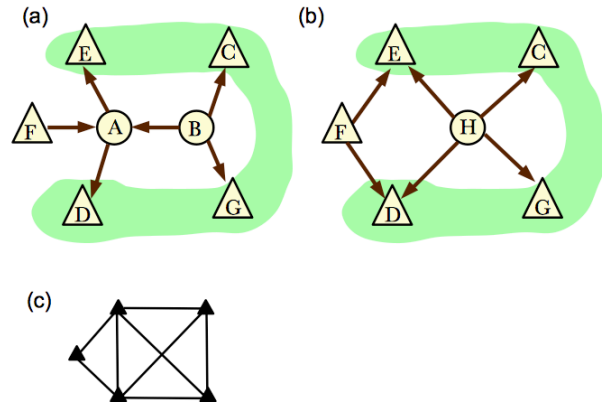


FIG. 4. Canonical projection of a GDAG. (a) shows the original GDAG, whose only maximal subset of size ≥ 2 is $\{C, D, E, G\}$ (highlighted). (b) is the corresponding canonical GDAG. By definition, both have the same skeleton, shown in (c).

(Note that what we call the canonical projection of G , Evans would call the ‘canonical DAG of the latent projection of G ’). As shown by Evans (see Proposition 4.9(b) and Theorem 4.13 in Ref. [15]), every GDAG is *observationally equivalent* to its canonical projection, in the sense that they have the same set of possible marginal distributions $P(V)$ on the observed variables.

Definition 6: GDAG skeleton.

Let $G(V, U)$ be a canonical GDAG with maximal connected subsets \mathcal{B} . The *skeleton* of G is defined to be an undirected graph having nodes V , and where two nodes are connected iff they are connected by an arrow in G , or belong to the same maximal connected subset in \mathcal{B} .

(If G is not canonical, we define its skeleton to be the skeleton of its associated canonical GDAG). Fig. 5 (a,b) shows two GDAGs with their corresponding skeletons underneath. We can now introduce the Skeleton method:

Theorem 1: The Skeleton method.

Consider a GDAG $G(V, U)$. Let $K(V, W)$ be a GDAG with the same set of observable variables V and observable CI relations $\text{CI}_G(V)$, but for which it is known that $\mathcal{C} = \mathcal{I}$ (assuming such a GDAG can be found). Suppose furthermore that the skeletons of G and K are different. Then $\mathcal{C} \subsetneq \mathcal{I}$ for G .

The proof follows from Proposition 5.6 in Ref. [15], which states that the observed marginals of G and K are different if they have different skeletons. Since they have the same set of observable variables and observable CI relations, the set \mathcal{I} is the same for both graphs, and

since $\mathcal{C} = \mathcal{I}$ for K , it follows that $\mathcal{C} \subsetneq \mathcal{I}$ for G . \square

This method is useful for GDAGs having few or no observed CI relations, where a suitable GDAG K is easy to find. For instance, if $\text{CI}_G(V) = \emptyset$, one can always take $K(V)$ to be a maximally connected DAG. It is likely to become increasingly difficult to find a suitable graph K with which to apply the Skeleton method for large numbers of variables; nevertheless the method works well for small GDAGs. Fig. 5 shows how it can be applied to graph #21 from Ref. [3], and the reader is encouraged to verify that the same method can be used to establish the interestingness of most of the other graphs considered by those authors. The notable exceptions are #2 (the Bell scenario), #8 (the Triangle scenario), and #15,16,20 which we consider in Sec. IV. For the Bell scenario, the method fails because there is no graph K that satisfies the no-signalling constraint and has $\mathcal{C} = \mathcal{I}$, while for the Triangle scenario it fails because the skeleton of all candidate K graphs is the same as that of G .

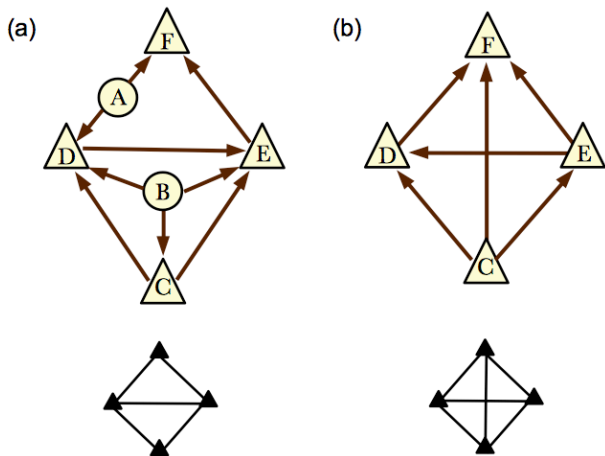


FIG. 5. Application of the Skeleton method to graph #21 from HLP. The original GDAG and its skeleton are shown in (a). Since the graph has no observable conditional independencies, a candidate for the comparison graph K is a complete graph, like the one shown in (b). Since its skeleton is different, Theorem 1 implies the original graph is not boring.

We now discuss a second graphical method by Evans [14], called the *E-separation method*.

Theorem 2 : The E-separation method.

Consider a GDAG G with observed CI relations $\text{CI}_G(V)$. Let X, Y, Z, W be disjoint sets of observable nodes, such that no member of Z is descended from W in the graph. Suppose that X and Y are d-separated by Z after deletion of W (and its connected arrows), and suppose $(X \perp Y|Z) \notin \text{CI}_G(V)$. Then $\mathcal{C} \subsetneq \mathcal{I}$ for G .

The proof follows from Theorem 4.2 in Ref. [14]. According to that theorem, there exists a constraint

on the distribution, and this constraint does not follow from the constraints $\text{CI}_G(V)$ when the latter excludes $(X \perp Y|Z)$. Hence there exists a non-independence constraint that is violated by some distribution in \mathcal{I} . (Note that non-trivial constraints only occur if X, Y, W are non-empty sets).

Fig. 6 shows how to apply the E-separation method to GDAG #17. Note that instead of $(F \perp D|C)$, we could alternatively have used the CI relation $(F \perp D)$, i.e. taking the conditioned set Z to be the empty set. On the other hand, we could *not* have deleted C and used the resulting relation $(F \perp D|E)$ to invoke E-separation, because E is descended from C , violating a premise of Theorem 2.

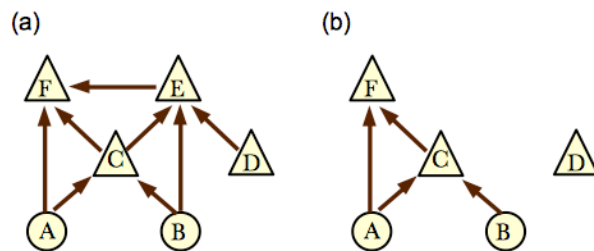


FIG. 6. Application of the E-separation method to graph #17 from HLP. The original GDAG is shown in (a), while (b) shows the GDAG after deleting E and its edges. Note (using d-separation) that the CI relation $(F \perp D|C)$ holds in (b) but not in (a), and that C is not descended from E . Theorem 2 then implies that the original graph is interesting.

For GDAGs of up to seven nodes, the E-separation method has similar success to the Skeleton method: the reader is encouraged to verify that it confirms the interestingness of all GDAGs considered by HLP except the usual suspects, namely the Bell scenario, the Triangle scenario, and the three GDAGs #15,16,20. It fails for the Bell scenario because there is no way to delete any observed nodes to create a CI relation that is not already implied by $\text{CI}_G(V)$. The Triangle scenario has a similar problem: to avoid triviality, one can only delete a single node, but then the remaining two nodes will still be correlated, i.e. no new CI relations are implied. The method fails for graphs #15,16,20, because the only viable candidates for the sets X, Y in Theorem 2 are nodes that cannot be d-separated by the deletion of other observed nodes.

Curiously, in the cases of up to seven nodes where the technique does work, the nodes corresponding to X, Y for the purposes of E-separation also correspond to the maximally correlated binary variables in the corresponding probability distribution found by HLP, for which a relevant Shannon-type entropic inequality is shown to be violated (note the highlighted nodes in Appendix D of Ref. [3]). Thus, although E-separation seems *a priori* to have little to do with entropic inequalities, the two

appear to be connected via this strange coincidence.

IV. ENTROPIC INEQUALITIES VIA ‘FINE-GRAINING’

We now turn to the problem of establishing the interestingness of the graphs # 15,16,20 as conjectured in HLP (these are displayed in Fig. 7).

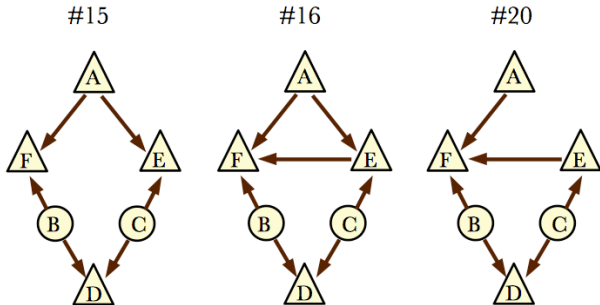


FIG. 7. The causal graphs #15,16,20 from HLP. These do not satisfy HLPs’ sufficient condition for boringness, but they also resist Evans’ sufficient criteria for interestingness. We find a probability distribution that violates the ‘fine-grained’ entropic inequality (3), thereby confirming that these graphs are indeed interesting.

Let us concentrate on graph #16; the others will follow in kind. For simplicity, we assume A is binary and takes values in $\{0,1\}$. Our goal is to demonstrate that the observed marginal of this graph is subject to an entropic constraint, namely:

$$I(E : D|\hat{A}_0) - I(F : D|\hat{A}_0) + I(F : D|\hat{A}_1) - I(E : D|\hat{A}_1) \leq H(D), \quad (3)$$

where the notation \hat{A}_0 means $\mathbf{do}(A = 0)$, i.e. ‘intervene on A and set it to 0’. Thus, for example, $I(E : D|\hat{A}_0)$ is the mutual information of E, D in the post-intervention distribution $P(E, D|\hat{A}_0)$. The reader might object that, if we cannot perform interventions, then we cannot obtain the quantities appearing on the left hand side of the inequality (3). In fact, we *can* obtain these quantities without doing an intervention, because A is an exogenous node in the graph (it has no parents). Hence the following identity holds:

$$P(E, D|\hat{A}_0) = P(E, D|A) \delta_{(A,0)}, \quad (4)$$

where $\delta_{(A,0)}$ is a Kronecker delta function. Intuitively, this says that the post-intervention distribution is the same as the distribution obtained by *post-selecting* on A having the particular value 0 or 1. We therefore have a situation where the causal graph allows us to learn something about the post-intervention distributions without

actually performing an intervention. Whenever a constraint such as the inequality (3) involves these post-intervention distributions, we call it a *fine-grained* constraint. We now establish a general framework for obtaining fine-grained entropic constraints from a causal graph, and use it to derive Eqn. (3).

A. Preliminaries

Let $P(R, X, Z)$ be a classical distribution (all variables are observed) compatible with some DAG $G(R, X, Z)$ in the usual sense that $\text{CI}_G(R, X, Z) \subseteq \text{CI}_P(R, X, Z)$. Here, X, Z are specific variables, R is the set of remaining variables, and Z is exogenous. Then the distribution factorises as $P(R, X, Z) = P(R, X|Z)P(Z)$. In the following we assume Z is binary for clarity, but the results can easily be extended to the case where Z is an arbitrary discrete variable. We give definitions for the case $Z = 0$; similar definitions are understood to hold for $Z = 1$.

Define the notation:

$$P(R, X|\hat{Z}_0) := P(R, X|\mathbf{do}(Z = 0)) = P(R, X|Z)\delta_{(Z,0)}. \quad (5)$$

For any subset of variables S (excluding Z), we define $H(S|\hat{Z}_0)$ as the entropy of S with respect to the post-intervention distribution $P(S|\hat{Z}_0)$:

$$H(S|\hat{Z}_0) := - \sum_S P(S|\hat{Z}_0) \log_2 [P(S|\hat{Z}_0)]. \quad (6)$$

Functions of the entropies, like the mutual information $I(X : Y|\hat{Z}_0)$, are defined analogously from the entropies of the post-intervention distribution. For example:

$$I(X : Y|\hat{Z}_0) := H(X|\hat{Z}_0) + H(Y|\hat{Z}_0) - H(XY|\hat{Z}_0). \quad (7)$$

Any CI relations that hold in the original distribution necessarily hold in the post-intervention distribution. For example, if $I(X : Y|Z) = 0$ holds in $P(X, Y, Z)$, then the statement $I(X : Y|\hat{Z}_0) = 0$ is also valid. Moreover, we have:

Corollary 3 :

If $(S \perp Z)$ holds in $P(S, Z)$, then $P(S|\hat{Z}_0) = P(S|\hat{Z}_1) = P(S)$.

This statement is a consequence of Rule 3 in Pearl’s *do calculus* (see Pearl [1], Theorem 3.4.1). It is important because it allows us to relate the entropies of distributions for which $Z = 0$ to entropies of distributions in which $Z = 1$, which implies fine-grained entropic constraints. In what follows, we only make use of Corollary 3, but in general the entire *do calculus* is available for deriving such constraints. We return to this point in Sec. IV C.

B. Derivation of the inequality

Returning to the specific case of graph #16, we aim to prove Eqn. (3). To this end we require the following elementary entropic inequalities:

$$H(DE) \leq H(E) + H(D), \quad (8)$$

$$H(E) + H(CDE) \leq H(CE) + H(DE), \quad (9)$$

$$H(DF) \leq H(F) + H(D), \quad (10)$$

$$H(F) + H(BDF) \leq H(BF) + H(DF), \quad (11)$$

$$H(D) + H(BCD) \leq H(CD) + H(BD), \quad (12)$$

as well as the CI relations:

$$(D \perp E|CA), \quad (13)$$

$$(D \perp F|BA), \quad (14)$$

$$(BCD \perp A), \quad (15)$$

$$(B \perp C), \quad (16)$$

which happen to hold in all three graphs. It is useful to define the quantities:

$$Q_0 := H(E|\hat{A}_0) - H(DE|\hat{A}_0);$$

$$R_0 := H(F|\hat{A}_0) - H(DF|\hat{A}_0);$$

$$Q_1 := H(E|\hat{A}_1) - H(DE|\hat{A}_1);$$

$$R_1 := H(F|\hat{A}_1) - H(DF|\hat{A}_1),$$

so that the LHS of (3) can be written (after expanding and cancelling some terms) as $Q_0 - R_0 + R_1 - Q_1$. From (9) & (13) we obtain:

$$H(E|\hat{A}_0) - H(DE|\hat{A}_0) \leq H(C|\hat{A}_0) - H(CD|\hat{A}_0), \quad (17)$$

and from (8) we obtain:

$$-H(D|\hat{A}_1) \leq H(E|\hat{A}_1) - H(DE|\hat{A}_1). \quad (18)$$

Similarly, from (11) & (14), and from (10) we obtain:

$$\begin{aligned} H(F|\hat{A}_1) - H(DF|\hat{A}_1) &\leq H(B|\hat{A}_1) - H(BD|\hat{A}_1) \\ -H(D|\hat{A}_0) &\leq H(F|\hat{A}_0) - H(DF|\hat{A}_0). \end{aligned} \quad (19)$$

It follows that:

$$\begin{aligned} Q_0 &\leq H(C|\hat{A}_0) - H(CD|\hat{A}_0); \\ -R_0 &\leq H(D|\hat{A}_0); \\ R_1 &\leq H(B|\hat{A}_1) - H(BD|\hat{A}_1); \\ -Q_1 &\leq H(D|\hat{A}_1). \end{aligned}$$

But (14) implies:

$$\begin{aligned} H(D|\hat{A}_0) &= H(D|\hat{A}_1) = H(D); \\ H(C|\hat{A}_0) - H(CD|\hat{A}_0) &= H(C) - H(DC); \\ H(B|\hat{A}_1) - H(BD|\hat{A}_1) &= H(B) - H(DB), \end{aligned} \quad (20)$$

so the LHS of (3) is subject to:

$$\text{LHS} \leq H(B) + H(C) - H(CD) - H(BD) + 2H(D). \quad (21)$$

Finally, using (12) and (16), this simplifies to:

$$\begin{aligned} \text{LHS} &\leq H(BC) - H(BCD) + H(D) \\ &\leq H(D), \end{aligned} \quad (22)$$

where in the last step we used the elementary inequality $H(BC) \leq H(BCD)$. This completes the proof of (3). \square

It follows that the entropic inequality (3) holds in graph #16; in fact, since the CI relations used in the proof are common to all three DAGs, the same inequality can be shown to hold in all three. Furthermore, we now present a probability distribution on the observed variables that satisfies all the observed CI relations but violates this inequality. Let $\tilde{P}(A, D, E, F)$ be an observed marginal distribution having the following properties:

- (i) all variables are binary with values in $\{0, 1\}$;
- (ii) the bits A and D are random and evenly distributed;
- (iii) $F = AD$;
- (iv) $E = (A \oplus 1)D$,

where \oplus is addition modulo 2. The distribution \tilde{P} has the special property that when $A = 0$, the bits E, D are perfectly correlated and F is fixed to 0, whereas when $A = 1$ the bits F, D are correlated and E is fixed. Although it satisfies all of the CI relations required by the DAGs #15, 16, 20 for the *observed* variables, it violates the constraint Eqn. (3), since (using the Shannon entropy) the LHS evaluates to 2, whereas the bound $H(D)$ for a binary variable D is only 1. Hence it cannot be a (classical) marginal of the underlying DAG. The existence of this distribution therefore establishes $\mathcal{C} \subsetneq \mathcal{I}$ for #15, 16, 20, completing HLP's analysis of DAGs with up to seven nodes.

C. Discussion

The method we employed in the previous section has the disadvantage that it still involves finding explicit inequalities and searching for a distribution that violates one of them. Fortunately, Wolfe et. al. recently proposed a convenient graphical method called the *inflation DAG* technique, with which they were independently able to establish the interestingness of GDAG #15, as well as the Triangle and Bell scenarios[20].

The distribution \tilde{P} described in the previous section is notable because it does not violate any standard Shannon-type entropic inequalities. In fact, the distribution lies inside an inner approximation of the entropy cone for scenario #15 (the author is indebted to Weilenmann and Colbeck for this information [21]). This means

that no conventional entropic inequality can distinguish it from a valid distribution for this scenario. We conclude that fine-grained inequalities are strictly more powerful than conventional entropic inequalities.

An interesting feature of graph #15 is that if we make A into an unobserved variable, we recover the Triangle scenario. It turns out that the marginal obtained by summing over A in \tilde{P} is *also* incompatible with the Triangle scenario [20]. This suggests that although the “W-distribution” discussed in Ref. [20] lies inside an inner approximation of the entropic cone for the Triangle scenario, it might be possible to distinguish it from a valid distribution using a fine-grained entropic inequality. However, since all observed variables in that scenario have parents, this would require an extension of the present formalism to non-exogenous nodes.

From the presentation given here, there seem to be two obvious ways to carry out this extension. The first method is to consider fine-graining by post-selecting on the values of non-exogenous nodes. For example, we could consider distributions of the form:

$$P(R, X|Z = 0) = \frac{P(R, X, Z) \delta_{(Z,0)}}{P(Z = 0)}, \quad (23)$$

which represents post-selecting on the outcome $Z = 0$ in the case where Z has parents in the DAG. This can be thought of as a generalisation of the RHS of Eq. (5) because it reduces to the same expression when Z is exogenous. Note, however, that for non-exogenous nodes the post-selected distribution $P(R, X|Z = 0)$ is not the same as the intervened distribution $P(R, X|\mathbf{do}(Z = 0))$.

This brings us to the second possible extension, already hinted at earlier in the paper: to use the concept of interventions. Specifically, we may consider post-intervention distributions like $P(R, X|\mathbf{do}(Z = 0))$ in more general situations where Z is not exogenous. One could then make use of the full *do calculus* in order to discover new fine-grained entropic inequalities. We leave it to future work to explore the potential of these extensions of the

fine-graining method.

V. CONCLUSIONS

The experimentally observed violation of Bell inequalities brings home the remarkable fact that, if we are certain that we know the causal structure of an experimental set-up, we can use it to make inferences about the fundamental laws of physics that govern the systems in the experiment. In particular, Bell-type experiments leverage the causal structure of space-time to rule out any faithful classical causal explanation of the experimental data. More generally, it would be useful to know which causal structures (represented by an associated GDAG) can be utilised for this purpose.

As pointed out in HLP, a necessary first step is to be able to identify the *boring* graphs, which cannot be used for distinguishing physical theories. Whereas HLP provided a sufficient condition for boringness, in this paper we drew attention to some necessary conditions due to Evans (namely, we pointed out that a graph can’t be boring if it violates Evans’ graphical criteria reviewed in Sec. III). Furthermore, we derived a fine-grained entropic inequality that is able to rule out the boringness of graphs #15,16,20. Inequalities of this type were shown to follow from Pearl’s *do calculus* of interventions, suggesting the possibility of a general method for deriving such inequalities in more complicated scenarios.

Acknowledgements: The author is grateful to Elie Wolfe and Rafael Chaves for helpful discussions, especially for pointing out the interesting properties of the distribution found in Sec. IV. This work has been supported by the European Commission Project RAQUEL, the John Templeton Foundation, FQXi, and the Austrian Science Fund (FWF) through CoQuS, SFB FoQuS, and the Individual Project 2462.

-
- [1] J. Pearl, *Causality: Models, Reasoning and Inference* (Cambridge University Press, 2000).
- [2] P. Spirtes, C. Glymour, and R. Scheines, *Causation, Prediction and Search*, Vol. 81 (Springer New York, 1993).
- [3] J. Henson, R. Lal, and M. F. Pusey, *New Journal of Physics* **16**, 113043 (2014).
- [4] J. Bell, *Epistemological Lett.* **9** (1976).
- [5] J. F. Clauser, M. A. Horne, A. Shimony, and R. A. Holt, *Phys. Rev. Lett.* **23**, 880 (1969).
- [6] N. Brunner, D. Cavalcanti, S. Pironio, V. Scarani, and S. Wehner, *Rev. Mod. Phys.* **86**, 419 (2014).
- [7] C. J. Wood and R. W. Spekkens, *New Journal of Physics* **17**, 033002 (2015).
- [8] M. Agnew, L. Vermeyden, D. Janzing, R. W. Spekkens, and K. J. Resch, *Nature Physics* **11**, 414 (2015).
- [9] M. S. Leifer and R. W. Spekkens, *Phys. Rev. A* **88**, 052130 (2013).
- [10] F. Costa and S. Shrapnel, arXiv:1512.07106 (2015).
- [11] J. Pienaar and Časlav Brukner, *New Journal of Physics* **17**, 073020 (2015).
- [12] B. S. Cirel’son, *Letters in Mathematical Physics* **4**, 93 (1980).
- [13] S. Popescu and D. Rohrlich, *Foundations of Physics* **24**, 379 (1994).
- [14] R. J. Evans, in *2012 IEEE International Workshop on Machine Learning for Signal Processing* (2012) pp. 1–6.
- [15] R. J. Evans, *Scandinavian Journal of Statistics* (2015), 10.1111/sjos.12194.
- [16] R. Chaves, L. Luft, T. O. Maciel, D. Gross, D. Janzing, and B. Schölkopf, *Proc. 30th Conf. UAI, AUAI Press*, 112 (2014), arXiv:1407.2256.
- [17] C. M. R. Chaves and D. Gross, *Nat. Commun.* **6** (2015), 10.1038/ncomms6766.
- [18] R. Chaves, L. Luft, and D. Gross, *New Journal of Physics*

- 16**, 043001 (2014).
- [19] M. Weilenmann and R. Colbeck, arXiv:1605.02078 (2016).
- [20] E. Wolfe, R. W. Spekkens, and T. Fritz, (in preparation)
- (2016).
- [21] Weilenmann and Colbeck, private communication.